

This article was downloaded by:

On: 21 January 2011

Access details: *Access Details: Free Access*

Publisher *Taylor & Francis*

Informa Ltd Registered in England and Wales Registered Number: 1072954 Registered office: Mortimer House, 37-41 Mortimer Street, London W1T 3JH, UK



## International Journal of Polymer Analysis and Characterization

Publication details, including instructions for authors and subscription information:

<http://www.informaworld.com/smpp/title~content=t713646643>

### Surface Morphology of Polymer Films Imaged by Atomic Force Microscopy

G. Julius Vancso<sup>a</sup>; Thomas D. Allston<sup>b</sup>; Ian Chun<sup>c</sup>; Leena-Sisko Johansson<sup>d</sup>; Guobin Liu<sup>a</sup>; Paul F. Smith<sup>e</sup>

<sup>a</sup> Faculty of Chemical Technology, University of Twente, AE Enschede, The Netherlands <sup>b</sup> Mobil Chemical Company, Films Division Research and Development Technical Center, Macedon, New York, USA <sup>c</sup> First Brands (Canada) Corporation, Orangeville, Ont., Canada <sup>d</sup> Materials Research, University of Turku, ElectroCity, Turku, Finland <sup>e</sup> Xerox Research Centre of Canada, Mississauga, Ont., Canada

**To cite this Article** Vancso, G. Julius , Allston, Thomas D. , Chun, Ian , Johansson, Leena-Sisko , Liu, Guobin and Smith, Paul F.(1996) 'Surface Morphology of Polymer Films Imaged by Atomic Force Microscopy', *International Journal of Polymer Analysis and Characterization*, 3: 1, 89 – 105

**To link to this Article:** DOI: 10.1080/10236669608032756

**URL:** <http://dx.doi.org/10.1080/10236669608032756>

PLEASE SCROLL DOWN FOR ARTICLE

Full terms and conditions of use: <http://www.informaworld.com/terms-and-conditions-of-access.pdf>

This article may be used for research, teaching and private study purposes. Any substantial or systematic reproduction, re-distribution, re-selling, loan or sub-licensing, systematic supply or distribution in any form to anyone is expressly forbidden.

The publisher does not give any warranty express or implied or make any representation that the contents will be complete or accurate or up to date. The accuracy of any instructions, formulae and drug doses should be independently verified with primary sources. The publisher shall not be liable for any loss, actions, claims, proceedings, demand or costs or damages whatsoever or howsoever caused arising directly or indirectly in connection with or arising out of the use of this material.

# Surface Morphology of Polymer Films Imaged by Atomic Force Microscopy

G. JULIUS VANCISO<sup>\*1</sup>, THOMAS D. ALLSTON<sup>2</sup>, IAN CHUN<sup>3</sup>,  
LEENA-SISKO JOHANSSON<sup>4</sup>, GUOBIN LIU<sup>1</sup>, PAUL F. SMITH<sup>5</sup>

<sup>\*1</sup>University of Twente, Faculty of Chemical Technology, P.O. Box 217, NL-7500 AE Enschede, The Netherlands, <sup>2</sup>Mobil Chemical Company, Films Division Research and Development Technical Center, Macedon, New York 14502, USA, <sup>3</sup>First Brands (Canada) Corporation, 101 John Street, Orangeville, Ont. L9W 2R1, Canada, <sup>4</sup>Materials Research, University of Turku, ElectroCity, Tykistökatu 4D, 20520 Turku, Finland, <sup>5</sup>Xerox Research Centre of Canada, 2660 Speakman Drive, Mississauga, Ont. L5K 2L1, Canada

(Received 11 October 1995; in final form 26 February 1996)

The surface morphology of commercial polymer films has been studied by contact mode and tapping mode atomic force microscopy. Flame-treated isotropic HDPE obtained by cast-film extrusion exhibited randomly oriented, 20–50-nm thick lamellar features of 200–400 nm in length, while uniaxially oriented films showed a shish-kebab-like morphology. The surface features of extrusion-blown films of blends of low-density polyethylene (LDPE) and linear low-density polyethylene (LLDPE) appeared as stacks of lamellae arranged in a cauliflower-like pattern. Images of isotactic polypropylene (PP) films obtained by cast-film extrusion consisted of branched fibrillar features. Corona treatment of the PP films resulted in the formation of 400–500 nm large “droplet-like” features at the surface. During metallization, 20–40-nm diameter Al particles were deposited. The metal layer formed followed the topography of the surface. The surface of ethylene-vinyl alcohol (EVOH) copolymer skins on PP consisted of radiating lamellae of 9–11 nm thickness. Contact mode AFM imaging of solvent-cast atactic polystyrene (PS) and polyvinylchloride (PVC) films induced surface erosion. During the scanning of PS and PVC films, wavy features formed with a predominantly perpendicular orientation with respect to the scan direction. The height of these features increased with plasticizer content from ca. 10 nm (unplasticized films) to over 100 nm. The height did not show any measurable relaxation over 24 h. This plastic deformation of the surface of the glassy polymer films studied is discussed. It is assumed that the glass-transition temperature of the outermost thin layer at the surface of glassy polymers is significantly lower than the bulk value.

---

Presented at the 8th International Symposium on Polymer Analysis and Characterization (ISPAC-8) held at Sanibel Island, Florida, May 22–24, 1995

*Keywords:* Atomic force microscopy; surface morphology; polymer films; plastic deformation; surface erosion of glassy polymers

## INTRODUCTION

Film applications constitute one of the largest uses of polymers. As the physical performance of film products strongly depends on the surface characteristics, the visualization of surface morphological features with submicron resolution is of particular technological interest. Morphologies resulting from the use of various processing methods used to produce commercial polymer films are only sparsely discussed in the literature. It is well known that quiescently crystallized bulk polymers usually exhibit hedritic and spherulitic structures. Crystallization under mechanical stress or orientation below the melting range can also result in fibrillar or epitaxial (e.g., shish-kebab) morphologies [1].

In order to understand and control the formation of typical surface morphological features of polymeric films, a number of important technological and scientific problems must be tackled. These include imaging and visualization of surface morphological features, relationships between surface morphology and structural features of the macromolecules, influence of the processing parameters on the formation of typical surface structures, and interrelations between the bulk and the surface morphologies. The majority of the information on surface morphologies of polymers available in the literature was obtained by electron microscopy. With the advent of various scanning force microscopy (SFM) techniques in the 1980s [2], a new family of surface characterization instrumentation for visualizing morphological features at film surfaces has become available. The resolution range of SFM, which is of particular interest for morphological studies, extends from the thickness of individual lamellae to the size of spherulites up to 100  $\mu\text{m}$ .

Some structural features of polymer films have already been imaged by SFM. Examples include oriented films of isotactic polystyrene [3], latex films [4], corona-treated polypropylene films [5], and melt-spun films of polyethylene and poly(butene-1) [6]. Further details can be found in review papers such as refs. [7] and [8].

Details of the SFM imaging techniques, including contact-mode atomic force microscopy (AFM) and non-contact tapping mode AFM are described in detail in the literature [2]. One of the most exiting features of

the AFM is that it allows one to image surfaces of polymers that exhibit structural order with molecular, or even atomic resolution in real space. The performance of the technique in studies of macromolecular packing, parameters of the crystal structure, chain disorder, and macromolecular conformation is discussed, for example in ref. [9]. In the present paper we focus our attention on scans with scan sizes between ( $500 \text{ nm} \times 500 \text{ nm}$ ) and ( $10 \text{ }\mu\text{m} \times 10 \text{ }\mu\text{m}$ ), and we describe surface morphological features without attempting to obtain molecular resolution. We present SFM images of polymer films that have technological interest, including isotropic and oriented high-density polyethylene (HDPE), blends of low-density polyethylene (LDPE) and linear low-density polyethylene (LLDPE), isotactic polypropylene (PP), multilayer PP / ethylene-vinyl alcohol (EVOH) copolymer structures, and solvent-cast films of glassy polymers such as atactic polystyrene (PS) and polyvinylchloride (PVC).

## EXPERIMENTAL

All SFM experiments reported in this paper were performed by NanoScope scanning probe microscopes manufactured by Digital Instruments (Santa Barbara, CA). AFM imaging was performed in the contact mode using NanoProbe  $\text{Si}_3\text{N}_4$  cantilevers with the exception of the images of blown PE and extrusion cast PP films. These were obtained in tapping mode experiments using rectangular NanoSensor Si cantilever probes of  $122\text{-}\mu\text{m}$  length and  $10\text{--}15\text{-}\mu\text{m}$  width. Information on the individual polymer systems is given below. The images shown correspond to raw data which were plane-fitted to correct for tilting. The high pass and the low pass filters were turned off during imaging.

## RESULTS AND DISCUSSION

### Polyethylene by Cast Film Extrusion

We investigated isotropic and uniaxially oriented HDPE films which were obtained by cast-film extrusion. The fine structure of extrusion-blown HDPE films was studied using high-resolution electron microscopy by Tagawa and Ogura [10]. Electron micrographs obtained by these authors unveiled a surface morphology consisting of "piled lamellar units" made up of three to ten

lamellar sheets. The piled lamellae were oriented predominantly perpendicularly to the machine direction in anisotropic films with uniaxial orientation. A comparison of this morphology and the structure we observed in extrusion-cast films helps to show differences in the surface structure which are caused by the different processing techniques.

In our studies, PP was coextruded with a thin layer of HDPE (approximately 1.0- $\mu\text{m}$  thickness). The total film structure was about 25- $\mu\text{m}$  thick. This multilayer structure was biaxially oriented using a tenter frame process which has been described in the literature [11]. The isotropic HDPE layer was produced by orienting this film while heating at temperatures above the melting range of HDPE (but below the melting range of PP). Subsequent to the solidification process, the HDPE surface of the films was flame-treated. The result was an essentially isotropic film with an exposed skin morphology as shown in Figure 1. During the flame treatment, details of the crystalline

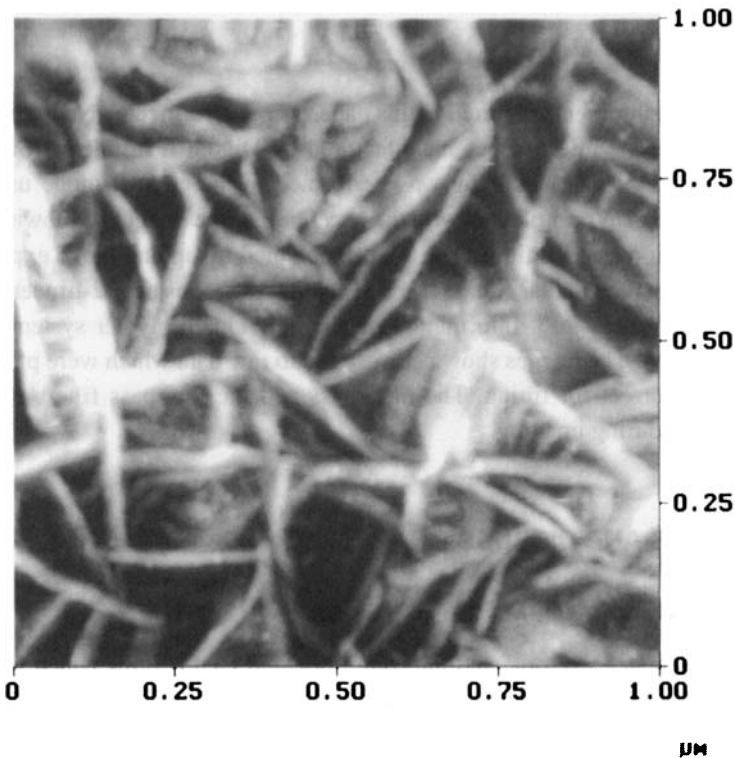


FIGURE 1 Contact-mode AFM image of extrusion-cast film of HDPE, flame treated, unoriented specimen.

skin morphology were exposed at the sample surface. The surface consisted of randomly arranged fibrillar features with a width in the order of 20–50 nm, and a typical length of 200–400 nm. These fibrils are consistent with images expected for predominantly edge-on lamellae, curved lamellae or stacks of lamellae. Due to the “convolution” of the AFM tip and the features imaged [12], the nanographs of the lamellae appear to be rounded, and the thickness obtained by direct observation of the distances between the fibrils is greater than the true thickness. The features seen on Figure 1 are consistent with images of curved individual lamellae and stacked lamellae consisting of a few crystals. It is interesting to point out that no predominant spherulitic or hedritic superstructure can be observed on the images. In addition, there is no indication of branched, piled-lamellar structure, as was presented in ref. [10].

Polymer films with a high degree of orientation were also obtained by stretching them in the machine direction, followed by orientation in the transverse direction at temperatures below the HDPE melting range. Flame-treated surfaces of these polymer films show a typical shish-kebab-like morphology, as can be seen in Figure 2 (scan size:  $2\ \mu\text{m} \times 2\ \mu\text{m}$ ). The crystalline core of the shish-kebab crystals, which consist of extended chains aligned in the MD direction, is horizontal in this micrograph. The “kebabs” consist of lamellar crystals overgrown epitaxially on the extended-chain “shishes” with typical apparent lamellar thickness in the range of 30–40 nm. The direction of the lamellar growth for the features shown in Figure 2 was vertical. Similar shish-kebab morphology which was captured by AFM was described earlier by Jandt et al. [13]. The lamellar thickness observed in our study of the commercial films imaged is slightly smaller than the value reported in ref. [13]. This is likely due to differences in the crystallization temperatures or to variations in the flatness of the lamellar crystals studied.

### **Polyethylene by Blown-Film Extrusion**

For the majority of end uses of PE films made by blown-film extrusion, optical clarity is of great importance, since this increases the appeal of the product. Optical performance can be specified by haze and gloss. Haze is that percentage of transmitted light which, in passing through the film specimen, deviates from the incident beam by more than  $2.5^\circ$  [14]. Gloss is measured by the intensity of light reflected from a specimen compared to a standard sample. We used atomic force microscopy to examine the inner

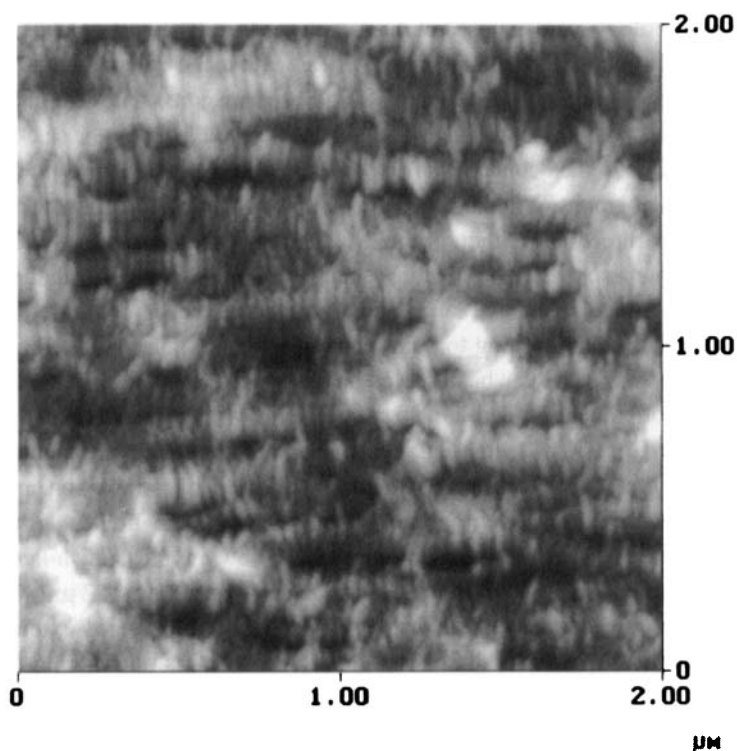


FIGURE 2 Contact-mode AFM image of extrusion-cast film of HDPE, flame treated, uniaxially oriented specimen.

and outer surfaces of commercial, blown PE films made of blends of LDPE and LLDPE. Using AFM, we obtained direct-space images of surface lamellae, and determined the surface roughness. A typical tapping mode AFM image of an as-blown film (scan size:  $10\ \mu\text{m} \times 10\ \mu\text{m}$ ) is shown in Figure 3. The film was oriented in the AFM such that the machine direction is placed vertically as viewed in the image. Typical images such as Figure 3 show packages of stacked lamellar features arranged in a cauliflower-like pattern. The typical feature thickness is in the range of 100 nm, which is too large for a single lamella. Therefore, the features imaged likely correspond to images of stacks of a few lamellae or twisted lamellae.

The haze of the films was also measured both before and after a suitable refractive index-matching oil was applied. In addition to the characterization of the surface morphology, these experiments allowed us to correlate haze,

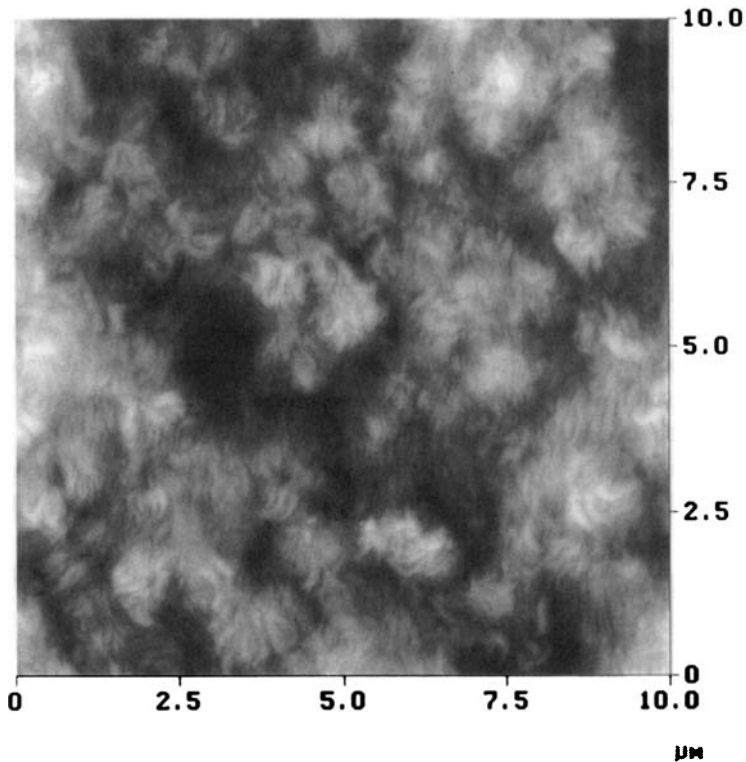


FIGURE 3 Tapping-mode AFM image of extrusion-blown film of an LLDPE-LDPE blend.

roughness and surface structure for films obtained at different processing conditions. Our results showed that raising the frost line height at constant extrusion temperatures increases the surface roughness, and furthermore these films also possess higher haze values. Further details together with orientation measurements are published in a separate study [15].

### **Polypropylene by Cast Film Extrusion**

AFM studies on the surface morphology of polypropylene films prior to, and after corona treatment have already been reported [5]. The focus of this work was to correlate the loss of adhesive strength of treated PP, and morphological changes observed at the surface by AFM. The formation of “droplet-like” features was observed which was attributed to local surface melting, or sublimation.



We performed studies on several industrial isotactic PP films. The untreated surface of biaxially oriented i-PP is characterized by a “branch-like” structure of fibrillar features that resembles an irregular, isotropic, cotton-like arrangement, as can be seen on Figure 4. A detailed image analysis showed that the branch-like structure originates from the polymer base sheet. Typical thickness values of fine fibers are ca. 100 nm. Corona treatment of these PP films results in the formation of “droplet-like” features measuring approximately 400–500 nm (see Figure 5). This observation confirms the results observed in ref. [5]. It is interesting to point out that for PE no formation of droplet-like features can be observed after flame treatment (see Figures 1 and 2). Instead, the morphological features of the crystallites are better exposed at the treated surface, so it is likely that the amorphous parts are “etched away” by the flame treatment.

Metallized PP films are used when specific barrier enhancement (e.g., light barrier) is needed, or when the appeal of the product (e.g., printability)

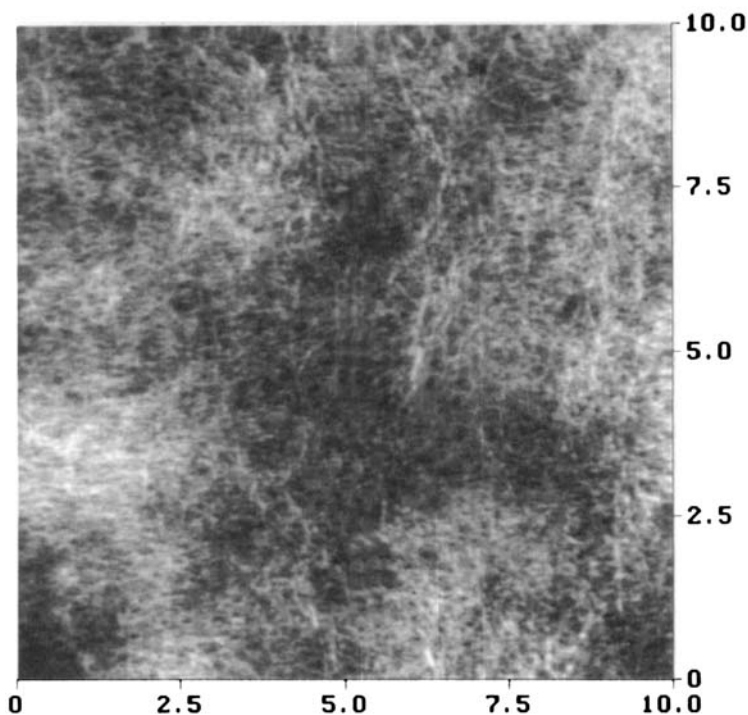


FIGURE 4 Tapping-mode AFM image of extrusion-cast, biaxially oriented, untreated PP film.

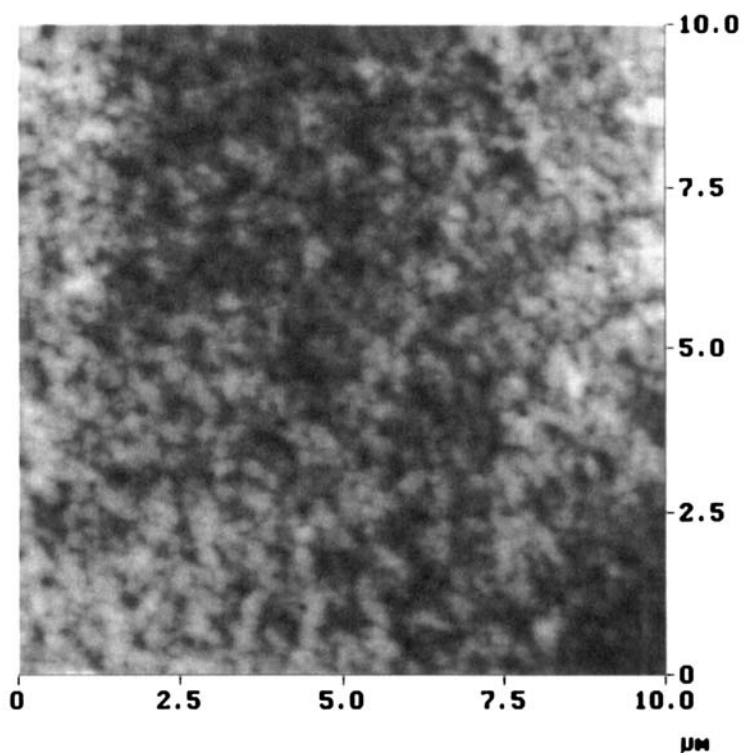


FIGURE 5 Tapping-mode AFM image of extrusion-cast, biaxially oriented, corona-treated PP film.

is important for marketing purposes. The surface morphology of metallized PP films was also studied by AFM. Typical aluminum grain sizes measured were in the range between 20–40 nm; that is, they appeared to be ca. one order of magnitude smaller than the size of the “droplet-like” features formed at the polymer surface during corona treatment. Our images showed that the metal layer follows the topography of the films, and the features of the non metallized films are not covered up.

### Ethylene-Vinyl Alcohol Copolymer by Cast Film Extrusion

EVOH copolymers with an alcohol content of 60–75 mol % offer excellent barrier properties, transparency, resistance against solvents, and good stability. They are easily processable by blown or cast extrusion as well as

coextrusion. The major uses of EVOH films include food packaging applications as well as use in multilayer structures for tubes, bottles, etc. [16]. The multilayer films studied and reported on here were biaxially oriented products which had a thickness of 25  $\mu\text{m}$  with a 1.0- $\mu\text{m}$  thick EVOH skin. The biaxial orientation of the PP film took place at temperatures that are high enough to melt the EVOH skin, similar to HDPE on PP.

Images of EVOH skins on PP are shown in Figure 6-8. As no EVOH images have been found in the literature, we show three micrographs displaying surface morphology at different magnification. The images exhibit a surface morphology that consists of radiating and stacked lamella-like features twisted around in a “cauliflower” arrangement which protrudes out of the film surface. There are similarities between these EVOH images and the features captured in the micrographs of extrusion-blown LLDPE-LDPE films (for a comparison see Figure 3). The high-resolution nanograph shown in Figure 8 (scan size: 500 nm  $\times$  500 nm) unveils fine details of the lamellar surface morphology. A quantitative analysis of the EVOH lamellar thickness yielded values in the range between 9.0 and 11.0 nm. It is interesting to mention that no features which correspond to flat-on or

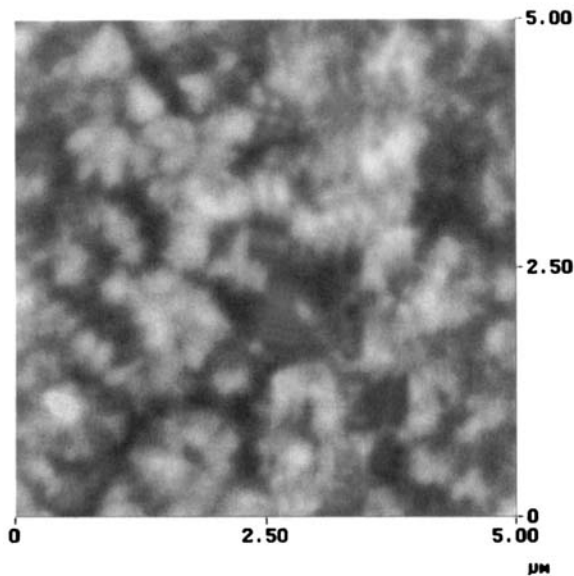


**FIGURE 6** Contact-mode AFM image of the EVOH skin on PP of a multilayer EVOH-PP film, corona treated.

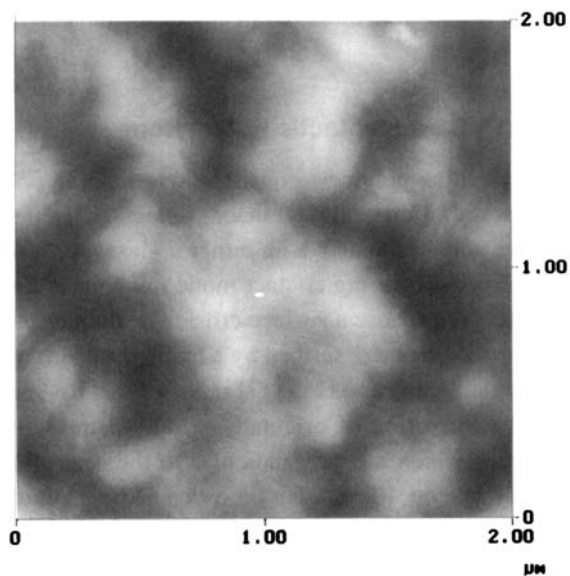


FIGURE 7 Medium magnification, contact-mode AFM image of the EVOH skin on PP of a multilayer EVOH-PP film, corona treated.

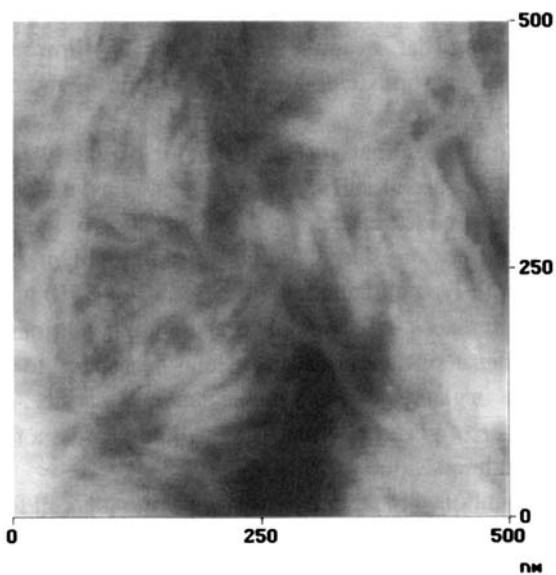


FIGURE 8 High magnification, contact-mode AFM image of the EVOH skin on PP of a multilayer EVOH-PP film, corona treated.

nearly-flat-on lamellae were observed in any of the lamella images shown in this paper.

### **Solvent-Cast PVC and Isotactic Polystyrene**

Films of noncrystalline polymers consist of overlapping polymer chains or can be composed of cross-linked macromolecules. Depending on the temperature, the polymer matrix is in either a glassy, or a rubbery state. Tip-surface interactions during contact mode imaging of the surfaces of “glassy” polymer films cause a surface erosion of the samples. This phenomenon was observed and described by a number of authors. In an early paper, for example, Leung and Goh [17] reported that tip-surface interactions lead to the formation of oriented periodic patterns of elongated, ridge-like features which are perpendicular to the scan direction at the surface of polystyrene films cast on mica. The “bundles” formed appeared to have a width in the order of 50 nm which increased during scanning. Similar observations were described independently by Meyers *et al.* [18]. These authors reported that the formation of the surface pattern depends on the polymer molar mass  $M$ , and becomes well defined and periodic for  $M$  values greater than the entanglement molar mass. This paper also gives an explanation for the formation of these surface erosion waves by assuming that, near the surface, the PS film behaves like a material which has, at room temperature, rubber-elastic rather than glassy behavior.

In addition to the peculiar surface behavior of glassy polymer films observed by AFM, careful surface roughness studies, using the virtually nonerosive tapping mode, reported on the observation of nanoscale “undulations” at the surface of a large number of glassy polymers [19]. These “undulations” with typical diameters in the order of 5–10 nm are present regardless of differences in the sample preparation conditions [19]. It was proposed that these surface undulations can be related to bulk heterogeneities present in glassy polymers on the nanometer scale. Assuming this is true, the surface of glassy polymer films would possess a finite, significant surface roughness value.

The results mentioned in the previous two paragraphs call for systematic scanning probe microscopy studies of films of amorphous polymers. In this paper we report on contact mode AFM studies of plasticized PS and polyvinylchloride (PVC). Detailed results are the subject of a forthcoming publication [20].

The PVC and PS samples used were purchased from Aldrich (Milwaukee, WI) and used without further purification. According to the supplier's information, the PVC had a "medium molar mass" and an inherent viscosity of 0.92 dL/g, and the PS sample had a weight average molar mass of 280,000 g/mol. We used dioctyl phthalate as plasticizer which was purchased from Aldrich. The polymer films were cast from THF solutions of 10 mg/mL concentration. Careful drying was essential in order to remove solvent traces which would act as plasticizer. Further details of the procedures followed will be published separately [20].

Figure 9 shows the first contact-mode AFM scan of an area of  $1\ \mu\text{m} \times 1\ \mu\text{m}$  on previously unscanned as-obtained PS film. The surface roughness is clearly visible on this image. The mean surface roughness,  $R_A$ , can be determined from AFM images, for example, by calculating the mean value of

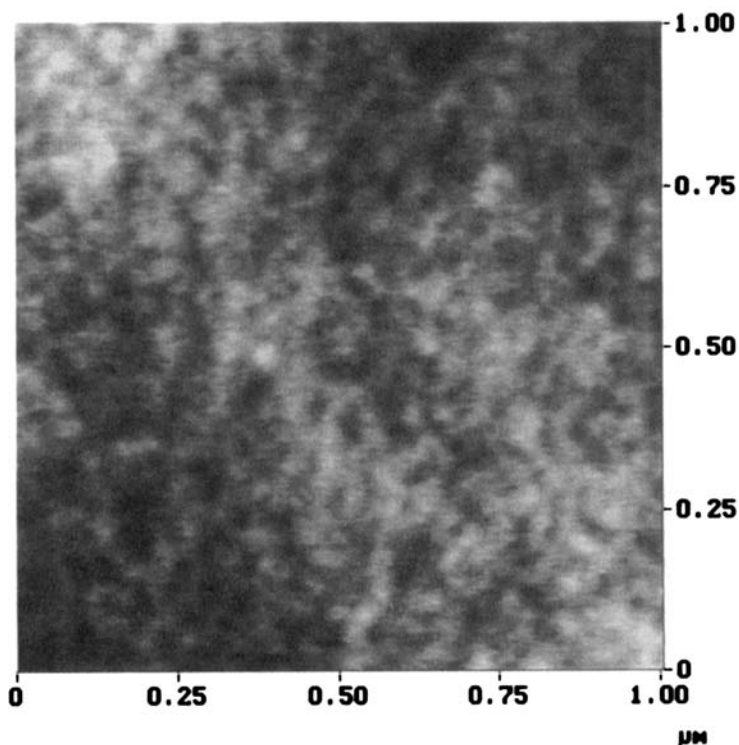


FIGURE 9 Contact-mode AFM image of a solvent-cast PS film, first scan, scanned at the lowest possible normal force near to pull-off.

the surface  $z = f(x,y)$  that was imaged relative to the center plane according to the following equation:

$$R_A = \frac{1}{L_x L_y} \int_0^{L_x} \int_0^{L_y} |f(x,y)| dx dy \quad (1)$$

where  $L_x$  corresponds to the scan size in the x direction, and  $L_y$  to the scan size in the y direction, respectively. The  $R_A$  values obtained by the NanoScope III used are corrected for the tilt of the center plane. The surface roughness observed by contact-mode AFM on typical first scans of as-cast polymer films with a size of ( $1 \mu\text{m} \times 1 \mu\text{m}$ ) to ( $2 \mu\text{m} \times 2 \mu\text{m}$ ) resulted in  $R_A$  values of  $0.30 \pm 0.05$  nm for PS, and  $1.3 \pm 0.2$  nm for PVC, respectively. Since the films were produced by using the same procedure in each case, this difference can not be related to specimen preparation. The features causing surface roughness observed in our contact-mode AFM micrographs have a typical diameter of 20–30 nm, and are thus ca. one order of magnitude greater than the typical feature size observed in the careful tapping mode AFM experiments of Kowalewski and Schaefer [19] on amorphous polymer films. Obviously, this difference is due to imaging different features. The larger typical feature size observed in our contact mode imaging is likely the result of the surface erosion and abrasion that takes place even during the first scan.

Figure 10 shows typical erosion patterns obtained on PS films. Along the diagonal connecting the bottom-left and the top-right corners of the image, two previously scanned areas of  $2 \mu\text{m} \times 2 \mu\text{m}$  size are visible. The  $5 \mu\text{m} \times 5 \mu\text{m}$  scan shown in Figure 10 was obtained by “zooming out” of the previously scanned areas and capturing the first scan. Figure 11 shows details of the surface erosion pattern formed on unplasticized PVC. The fibrous features in the perpendicular direction to the (horizontal) scan direction are clearly visible. The ridges protrude out of the film surface while the valleys in between are carved into the film.

We performed contact-mode AFM scanning on PS and PVC films with different plasticizer content and at different normal forces (i.e., at different scanning setpoint values). Without plasticizer, the amplitude of the wavy features after 1 h of scanning was in the range of 10–40 nm, depending on the force used. At plasticizer contents that decrease the value of the glass-transition temperature  $T_g$  close to room temperature, the ridge amplitude shows a dramatic increase and reaches values over 100 nm. We observed no height relaxation of the wavy features over a period of 24 h. Thus one

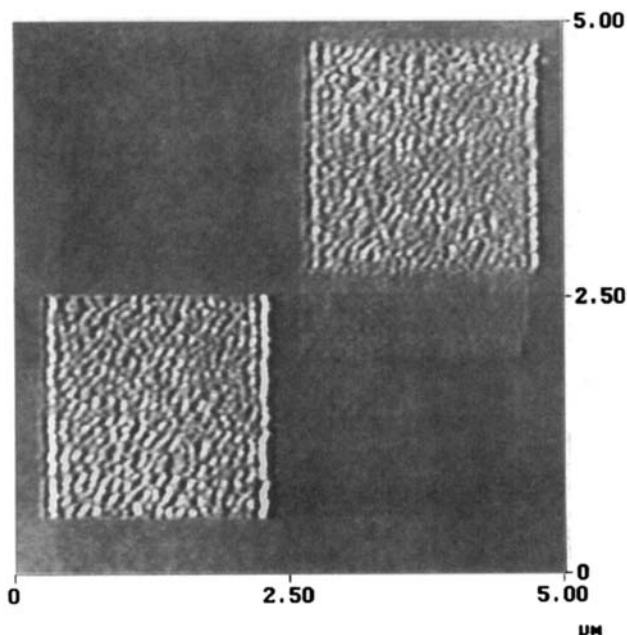


FIGURE 10 Contact-mode AFM image of a solvent-cast PS film showing two patterns of erosion previously scanned over a period of 1 h. The micrograph shown was captured immediately after zooming out of the previously scanned and eroded area.

can assume that the top layer of polymer films can be deformed as a plastic body, and therefore the localized deformation will not be recovered upon the release of the stress. Other characteristics of the wavy ridges include a linear dependence between the feature height and the spacing between the waves which formed while we found no dependence of the scanning speed on the characteristics of these features.

The formation of the wavy features described above is consistent with the existence of a thin top layer at the polymer film which does not have glassy properties, even though the bulk of the film is in the glassy state. Keddie et al. [21] recently reported that the  $T_g$  value of thin films of PS and poly(methyl methacrylate) (PMMA) decrease as the thickness of the films  $d$  is reduced. The data was fitted to the analytical function that contains the bulk glass-transition temperature  $T_g(\infty)$ , a material-characteristic length constant  $A$ , and an exponent  $\delta$ , and is written in the following form:

$$T_g(d) = T_g(\infty)[1 - (A/d)^\delta] \quad (2)$$



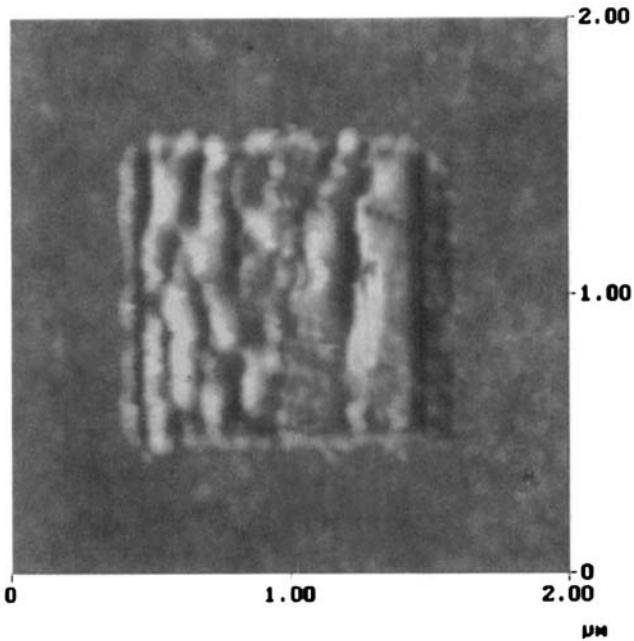


FIGURE 11 Contact-mode AFM image of a solvent-cast PVC film showing a patterns of erosion previously scanned over a period of 1 h. The micrograph shown was captured immediately after zooming out of the previously scanned central area.

If we assume a two-phase model for our polymer films, that is, if they consist of a thin, ideal plastic layer with a thickness  $d$ , and a glassy bulk, then the  $d$  value can be estimated from Equation (2). For PS films, the best fit to the data was obtained using  $T_g(\infty) = 373.8$  K,  $A = 3.2$  nm, and  $\delta = 1.8$  [21]. By using these parameters in equation (2), we obtained a value of  $d = 7.8$  nm for the thickness of the plastic layer at the surface of glassy PS films at room temperature. This value is in the same range as the half-amplitude of the wavy features observed, for example, in Figures 10 and 11. It can be assumed that this plastic layer at the film surface gets deformed due to tip-sample interaction during AFM scanning. An increase of the plasticizer content results in an increase of the thickness of the plastic layer at the film surfaces, and, as a result, the amplitude of the ridges observed increases.

In summary, the AFM results obtained in this section are consistent with the existence of a thin plastic layer at the surface of glassy polymer films. The thickness of this plastic layer was found to increase with the plasticizer content, that is, with the decrease of the bulk glass transition temperature.

## Acknowledgment

The authors are grateful for the financial support given by the Ontario Centre for Materials Research, the Natural Sciences and Engineering Research Council of Canada, the Mobil Chemical Company, First Brands (Canada) Corporation, the University of Toronto, and the University of Turku.

## References

1. E. Woodward, *Understanding Polymer Morphology*; Hanser: Munich, 1995; Chapter 6.
2. The AFM was invented and described by G. Binnig, C. F. Quate, and Ch. Gerber, *Phys. Rev. Lett.*, **56**, 930 (1986). The various imaging modes used in polymer research are described for example, by M. J. Miles In *Characterization of Solid Polymers*; Ed. S. J. Spells, Ed., and Chapman & Hall: New York, 1994; pp 17–55.
3. K. D. Jandt, L. M. Eng, J. Peterman, and H. Fuchs, *Polymer*, **33**, 5331 (1992).
4. Y. Wang, D. Juhué, M. A. Winnik, O. M. Leung, and M. C. Goh, *Langmuir*, **8**, 760 (1992).
5. R. M. Overney, R. Lüthi, H. Haefke, J. Frommer, E. Meyer, H.-J. Güntherodt, S. Hild, and J. Fuhrmann, *Appl. Surf. Sci.*, **64**, 197 (1993).
6. M. J. Miles, K. D. Jandt, T. J. McMaster, and R. L. Williamson, *Colloids Surf.*, **A 87**, 235 (1994).
7. M. C. Goh, *Adv. Chem. Phys.* Vol. **91**, p 1, 1995.
8. V. V. Tsukruk and D. H. Reneker, *Polymer*, **36**, 1791 (1995).
9. D. Snétivy and G. J. Vancso, *Colloids Surf.*, **A87**, 257 (1994).
10. T. Tagawa and K. Ogura, *J. Polym. Sci.; Polym. Phys. Ed.*, **18**, 971 (1980).
11. C. J. Benning, *Plastic Films for Packaging*; Techomic: PA, 1983; pp 21–23.
12. G. J. Vancso, R. Nisman, D. Snétivy, H. Schönherr, P. Smith, C. Ng, and H. Yang, *Colloids Surf.*, **A87**, 263 (1994).
13. K. D. Jandt, M. Bukh, M. J. Miles, and J. Peterman, *Polymer*, **35**, 2458 (1994).
14. *Encyclopedia of Polymer Science*, J. I. Kroschwitz, Ed.; Wiley: New York, 1987; Vol. 7, p 85.
15. P. F. Smith, I. Chun, G. Liu, D. Dimitrievich, J. Rasburn, and G. J. Vancso, *Polym. Eng. Sci.*, in press.
16. *Encyclopedia of Polymer Science and Engineering*; J. I. Kroschwitz, Ed.; Wiley: New York, 1985; Vol. 2, p 188.
17. M. Leung and M. C. Goh, *Science*, **255**, 64 (1992).
18. G. F. Meyers, B. M. DeKoven, and J. T. Seitz, *Langmuir*, **8**, 2330 (1992).
19. T. Kowalewski and J. Schaefer, IUPAC MacroAkron Conference Abstracts, The University of Akron, 1994; O-6.1-4M, p 781.
20. L. S. Johansson and G. J. Vancso manuscript in preparation.
21. J. L. Keddie, R. A. L. Jones, and R. A. Corie, *Europhys. Lett.*, **27**, 59 (1994); J. L. Keddie, R. A. L. Jones, and R. A. Corie, *Faraday Discuss.*, **98**, 219 (1994).